forests

MDPI

Article

Warming Effects on *Pinus sylvestris* in the Cold–Dry Siberian Forest–Steppe: Positive or Negative Balance of Trade?

Tatiana A. Shestakova [1,2,*], Jordi Voltas [1], Matthias Saurer [3], Rolf T. W. Siegwolf [4] and Alexander V. Kirdyanov [5,6]

1 Department of Crop and Forest Sciences—AGROTECNIO Center, University of Lleida, Avda. Rovira Roure 191, 25198 Lleida, Spain; jvoltas@pvcf.udl.cat
2 Mathematical Methods and IT Department, Siberian Federal University, St. L. Prushinskoy 2, 660075 Krasnoyarsk, Russia
3 Swiss Federal Institute for Forest, Snow and Landscape Research (WSL), Zürcherstrasse 111, 8903 Birmensdorf, Switzerland; matthias.saurer@wsl.ch
4 Laboratory of Atmospheric Chemistry, Paul Scherrer Institute (PSI), 5232 Villigen, Switzerland; rolf.siegwolf@psi.ch
5 Sukachev Institute of Forest, Akademgorodok 50/28, 660036 Krasnoyarsk, Russia; kirdyanov@ksc.krasn.ru
6 Institute of Ecology and Geography, Siberian Federal University, Pr. Svobodny 82, 660041 Krasnoyarsk, Russia
* Correspondence: tasha.work24@gmail.com; Tel.: +34-973-702-522

Received: 10 November 2017; Accepted: 5 December 2017; Published: 7 December 2017

Abstract: Understanding climate change impacts on drought-prone forests is a critical issue. We investigated ring-width and stable isotopes ($\Delta^{13}C$ and $\delta^{18}O$) in two *Pinus sylvestris* stands of the cold–dry Siberian forest–steppe growing under contrasting climatic trends over the last 75 years. Despite regional warming, there was increasing precipitation during the growing period at the southern site (MIN) but increasing water deficit (WD) at the northern site (BER). Intrinsic water use efficiency (WUE_i) increased similarly (ca. 22%) in response to warming and rising atmospheric CO_2. However, the steady increase in WUE_i was accompanied by divergent growth patterns since 1980: increasing basal area increment (BAI) in MIN (slope = 0.102 cm^2 $year^{-2}$) and decreasing BAI in BER (slope = −0.129 cm^2 $year^{-2}$). This suggests that increased precipitation, mediated by CO_2 effects, promoted growth in MIN, whereas intensified drought stress led to decreased carbon gain and productivity in BER. When compared to warm–dry stands of eastern Spain, the WUE_i dependence on WD was three-fold greater in Siberia. Conversely, BAI was more affected by the relative impact of water stress within each region. These results indicate contrasting future trajectories of *P. sylvestris* forests, which challenge forecasting growth and carbon sequestration in cold–dry areas.

Keywords: climate warming; dendroecology; drought stress; forest–steppe; Scots pine; Central Siberia; stable isotopes; tree rings

1. Introduction

Scots pine (*Pinus sylvestris* L.) is the world's most widespread conifer as it can be found throughout Eurasia from the western Mediterranean to the Russian Far East. Such vast distribution encompasses a broad array of climates, including the frequent and severe summer droughts of southern Iberian Peninsula and the fiercely cold winters of north-eastern Siberia [1,2]. Climate variability has indeed been a fundamental player shaping the species adaptive structure in terms of drought tolerance [3] and cold hardiness [4]. Although growth of Scots pine is essentially limited by low temperatures in boreal forests [5–7], large areas in southern Siberia also have low precipitation and are therefore cold and dry.

These transition forests (forest–steppe belt) represent the ecotone between the boreal taiga to the north and the steppe grasslands to the south where productivity is simultaneously limited by low temperatures (by severely confining the active growing season) and water availability (by challenging tree performance during the short growing period) [8].

Global climate change is placing increasing pressure on forest ecosystems from virtually all regions over the globe [9–12]. In the case of Scots pine, growth can be promoted by increased temperatures at its northern and upper distribution limits where productivity is primarily cold-limited [6,13]. In contrast, decrease in productivity, reversal of carbon balance and even large-scale dieback episodes have already been observed in the southern, warm habitats of the species [14–17]. Moreover, there is growing evidence that some cold-constrained sites may be progressively affected by drought stress under warmer conditions due to exacerbated soil moisture deficit linked to decreased precipitation or increased evapotranspirative demand during the vegetative period [18–20]. Such opposing influences of low temperatures and drought on growth dynamics bring much uncertainty about species vigor and productivity across the whole distribution range [2,16] and, particularly, in cold–dry environments [21]. Besides, other dry environments typical of warmer regions such as the Mediterranean, where Scots pine is found at high altitudes, are also subjected to winter cold and summer droughts [22]. In this regard, the comparison of the simultaneous effects of low temperatures and drought on Scots pine performance near its trailing edge at cold (i.e., Siberian forest–steppe) and at warm environments (i.e., Mediterranean mountains) is of special interest to forecast climate change impacts on conifer forests.

Tree rings are extensively used to assess climate change effects on forest ecosystems [23]. Most dendroecological studies infer long-term changes in tree performance based on radial growth patterns. However, additional information on leaf-level physiology can be gained through the analysis of stable isotopes in tree rings [24]. On the one hand, carbon isotope discrimination ($\Delta^{13}C$) depends on factors affecting CO_2 assimilation, as expressed in the ratio of photosynthetic rate to stomatal conductance (A/g_s or intrinsic water use efficiency) [25]. On the other hand, oxygen isotope composition ($\delta^{18}O$) is mainly influenced by source water isotopic composition (i.e., precipitation modulated by residence time in soil and associated evaporation effects) and leaf water enrichment due to transpiration at the stomata [26]. Both isotope types are therefore linked via effects at the leaf level mediated through changes in stomatal conductance caused by varying soil moisture and atmospheric evapotranspirative demand [27]. As $\delta^{18}O$ is not influenced by photosynthetic processes, combining $\Delta^{13}C$ and $\delta^{18}O$ may allow separating stomatal and photosynthetic effects on tree performance, which may eventually determine changes in productivity [28,29].

Despite pinewoods of the forest–steppe zone of Central Siberia receiving increasing attention [30–33], the ecophysiological responses of Scots pine to current climate change in this region remain poorly investigated. Here, we assess climate effects on physiological processes underlying tree growth patterns in two contrasting sites with regard to climate trends that are located near the moisture limit of the species range at the southern edge of the boreal forest belt. This area offers an excellent opportunity to test for global change impacts on forests growing under the combined effects of low temperatures and water scarcity [34]. These interactions may expose trees to previously untested bioclimatic envelopes, perhaps resulting in a relaxation of cold limitation modifying phenology and an exacerbation of drought effects impacting on carbon and water budgets. In contrast to the large-scale warming trend, local rainfall patterns in this region display significant spatial variability [35,36], which may lead to a differential vulnerability of these stands to fluctuations in the moisture regime during the short growing season. Based on these premises, the aim of this study was to understand how *P. sylvestris* forests have responded to divergent climatic changes observed during the last 75 years in the region through the combined analysis of ring-width and stable isotopes. We hypothesized that climatically-induced spatial variation in water availability determines the ecophysiological responses and tree growth of Scots pine populations in cold–dry environments of the Siberian forest–steppe ecotone and, ultimately, their responses to the ongoing temperature rise. In particular, we assumed that WUE_i was uncoupled from changes in secondary growth in spite of divergent climate trends at the site level (increasing warming-induced drought stress vs. enhanced water availability and

relaxation of cold limitation). Our specific objectives were (i) to examine how climatic variability is reflected in tree-ring traits (ring-width, carbon, and oxygen isotopes) of Scots pine growing under a varying level of progressive exposition to drought stress in cold–dry areas; (ii) to evaluate trends in tree growth (basal area increment, BAI) at stand level and how changes in productivity are potentially linked with convergent physiological responses (i.e., increased WUE_i); and (iii) to disentangle climate drivers controlling tree performance of these cold–dry forests and assess whether recent changes in local climate and CO_2 have modulated tree responses to drought stress during the growing period. Furthermore, and in order to compare Scots pine responses in cold–dry areas with those of other dry environments typical of warmer regions, we complemented our data with growth and WUE_i records compiled in a previous study [37] in which *P. sylvestris* was sampled in two high-altitude Mediterranean stands of the eastern Iberian Peninsula.

2. Materials and Methods

2.1. Study Sites

The study was conducted in two sites located 157 km apart in the northern edge of Altai–Sayan ecoregion in the south of Central Siberia (Russia). The region belongs to the forest–steppe belt which is bounded by the Siberian taiga in the north and the Mongolian grassland steppe in the south (Figure 1a). The northern stand (Berenzhak site, BER; 54°16′ N, 89°37′ E) is formed on a gentle south-facing slope in the south-east of the Kuznetsk Alatau mountain range (615–621 m a.s.l.) (Table 1). BER is an open mixed pine (*P. sylvestris*)–larch (*Larix sibirica*) forest with presence of scattered birch (*Betula pendula*) on a gray mountain soil. The southern stand (Malaya Minusa site, MIN; 53°43′ N, 91°50′ E) is situated at the edge of a belt pine forest in the north of Minusinsk Depression (320–338 m a.s.l.) (Table 1). MIN is an open monospecific pine forest with admixture of birch growing on a sandy soil with a humus layer of 8–10 cm. Both stands have experienced minimal land use pressures (e.g., logging, grazing) over the 20th century [38].

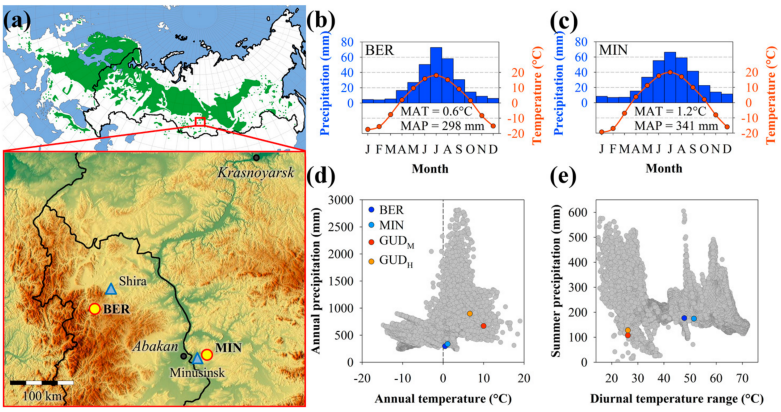

Figure 1. Geographical location and climatic characteristic of the sampling sites in the forest–steppe of Central Siberia. (**a**) *P. sylvestris* distribution (green shading; [39]) and location of the study area (**top**) and distribution of pine stands (**bottom**). Circles mark positions of the sampling sites and triangles denote Minusinsk and Shira meteorological stations used in the analyses. (**b**,**c**) Climate diagrams corresponding to northern (BER) and southern (MIN) sites. The primary *y*-axis indicates monthly precipitation (bars) and the secondary *y*-axis monthly mean temperature (lines). Average monthly values of climate factors were estimated based on the climate data from the nearest meteorological stations for the period 1940–2014. The mean annual temperature (MAT) and mean annual precipitation (MAP) are given for each site. (**d**,**e**) Autoecology diagram of *P. sylvestris* distribution with sites used in the analyses depicted as colored circles: blue—BER (cold–dry site), light blue—MIN (cold–moist), red—GUD_M (warm–dry) and orange—GUD_H (warm–moist) (see Section 2.6. for further details on GUD sites). The species range is derived from the EUFORGEN distribution map (http://www.euforgen.org/species/pinus-sylvestris).

The region is characterized by a moderately cold and dry continental climate with complex topography (mountain slopes, flats, depressions, etc.), which determines a wide diversity of local conditions. To characterize stand growing conditions, we obtained climate data from the nearest meteorological station to each study site, Shira (54°30′ N, 89°56′ E; 475 m a.s.l.) and Minusinsk (53°43′ N, 91°42′ E; 254 m a.s.l.) (Figure 1a), which are located at a distance of 33 km and 9 km from BER and MIN, respectively. According to the meteorological data, mean annual temperature is slightly higher in MIN (1.2 °C) than in BER (0.6 °C), with January being the coldest month (mean temperature = −19.3 °C for MIN and −17.3 °C for BER) and July the warmest month (+19.9 °C for MIN and +18.0 °C for BER) (period 1940–2014). The growing season, defined as the period with mean air temperature above 10 °C [40], starts at the end of April (MIN) or beginning of May (BER) and spans for 110–120 days on average (till end of August, approximately). Mean annual precipitation is lower in BER (298 mm) than in MIN (341 mm), with up to 70% occurring from May to August in both sites (Figure 1b,c). Although precipitation peaks during the growing period, potential evapotranspiration (PET) is over 2.5-fold greater than water supply during these months (PET = 502 mm for BER and 522 mm for MIN; [41]), hence resulting in recurrent summer droughts in the region.

Table 1. Geographic and dendrochronological characteristics of the sampling sites. Abbreviations: EPS, Expressed Population Signal; Rbar, mean inter-series correlation; TRW, tree-ring width; $\Delta^{13}C$, carbon isotope discrimination; $\delta^{18}O$, oxygen isotope composition. The mean values of tree-ring traits are estimated over the period 1940–2014 and the variability is expressed as standard deviation (±SD). The statistical significance of the differences in tree-ring mean values is also provided according to two-tailed Student's *t*-test.

Site	Code	Latitude (N)	Longitude (E)	Altitude (m a.s.l.)	Nr Trees [1]	Time Span	EPS > 0.85	Rbar [2]	TRW ± SD (mm)	$\Delta^{13}C \pm SD$ (‰) [3]	$\delta^{18}O \pm SD$ (‰) [3]
Berenzhak	BER	54°15′41″	89°37′26″	615–621	20/19	1830–2014	1846	0.56	1.28 ± 0.42	15.82 ± 0.80	27.45 ± 0.83
Malaya Minusa	MIN	53°43′25″	91°50′24″	320–338	20/17	1899–2014	1902	0.48	1.49 ± 0.45	16.09 ± 0.62	28.51 ± 0.88
Two-tailed Student's *t*-test (*p*-value)									<0.01	<0.05	<0.001

[1] Number of trees (sampled/cross-dated); [2] Study period (1940–2014); [3] For five trees used for isotope analysis.

2.2. Field Sampling and Tree-Ring Measurements

Field work was conducted at the end of August 2014. Twenty mature, dominant, and healthy trees were randomly selected at each site. The average age of the trees was 116 ± 35 years (mean ± SD) in BER and 94 ± 11 years in MIN. Two cores from the same cross-slope side of the trunk were extracted at breast height with a 5-mm-diameter increment borer. Samples were oven-dried at 60 °C for 48 h and one core per tree was sanded with sandpapers of progressively finer grain until tree rings were clearly visible. The remaining core of every tree was kept intact for isotope analyses. Tree rings were visually cross-dated and measured with precision of 0.01 mm using a Lintab system (Rinntech, Heidelberg, Germany). Cross-dating was verified with the COFECHA program [42]. Poor samples failing to pass the cross-dating check were discarded for chronology developing (one ring-width series in BER and three in MIN).

In order to build indexed tree-ring width chronologies (TRW_i) for each site, the individual series were first standardized using a cubic-smoothing spline curve of 50 years with a 50%-frequency response cut-off. This procedure minimizes the effect of biological trends (e.g., tree age) and disturbances (e.g., fire scars) on radial growth, hence preserving high-frequency variability potentially related to climate [43]. Standardization converted ring-width measurements into dimensionless indices with mean value of 1 and constant variance. Next, autoregressive models were applied to remove the first-order temporal autocorrelation in the detrended series and produce residual or pre-whitened indices. Finally, a biweight robust mean was computed to provide indexed chronologies for each site (Figure 2a,b). These procedures were done using the ARSTAN program [44]. The reliability of ring-width chronologies for capturing the hypothetical population signal was checked against the expressed population signal (EPS) criterion with a threshold value of 0.85 [45]. Inter-series correlation

(Rbar) statistics and Principle Component Analysis (PCA) were used to estimate the internal coherence of each chronology [45]. These statistics were calculated over the period 1940–2014, when the sample size was largest and growth had stabilized (i.e., excluding years of juvenile phase).

To characterize the absolute radial growth trends at each site, tree-ring width measurements were transformed to basal area increment (BAI). BAI represents an accurate indicator of tree vigor and growth over time because it accounts for the variation caused by adding volume to a circular stem [46]. On the other hand, it relies on the assumption of near-perfect circular and centered trunk sections, which was approximately met in both sites. BAI was calculated from the set of cross-dated tree-ring width series according to

$$\mathrm{BAI} = \pi(R_t^2 - R_{t-1}^2) \quad (1)$$

where R is the radius of the tree and t is the year of tree-ring formation. Finally, we calculated a mean BAI chronology for each site (Figure 2c,d). Trends in BAI were assessed independently for two consecutive periods (1940–1979 and 1980–2014) using linear regressions.

2.3. Stable Isotope Analyses

The five best cross-dated trees per site were selected for isotope measurements. Tree rings were split from the intact cores with annual resolution for the period 1940–2014. Rings corresponding to the same year and site were pooled into a single sample before analysis [47]. Every 10 years (1944, 1954, etc.), rings were analyzed individually to estimate between-tree variability in the isotope signals. The resulting samples were homogenized with a ball mill (Retsch, Haan, Germany) and purified to α-cellulose following [48].

For carbon isotope analysis, 0.4–0.6 mg of dry α-cellulose was weighed into tin foil capsules and combusted using a Flash EA-1112 elemental analyzer (Thermo Fisher Scientific Inc., Waltham, MA, USA) interfaced with a Finnigan MAT Delta S isotope ratio mass spectrometer (Thermo Fisher Scientific Inc.). For oxygen isotope analysis, 0.8–1.0 mg of dry α-cellulose was weighed into silver foil capsules and pyrolyzed using a Pyrocube thermal conversion/elemental analyzer (Elementar, Hanau, Germany) interfaced with a Finnigan Deltaplus XP isotope ratio mass spectrometer (Thermo Fisher Scientific Inc.). Isotope ratios were expressed as per mil deviations using the δ notation relative to Vienna Pee Dee Belemnite standard (for carbon) and Vienna Standard Mean Ocean Water (for oxygen) standards. The accuracy of the analyses (SD of working standards) was 0.1‰ ($\delta^{13}C$) and 0.2‰ ($\delta^{18}O$).

To account for changes in $\delta^{13}C$ of atmospheric CO_2 ($\delta^{13}C_{air}$), we calculated carbon isotope discrimination ($\Delta^{13}C$) from $\delta^{13}C_{air}$ and wood $\delta^{13}C$ ($\delta^{13}C$) (Figure 2e,f) following [25]

$$\Delta^{13}C = \frac{\delta^{13}C_{air} - \delta^{13}C}{1 + \delta^{13}C/1000} \quad (2)$$

$\delta^{13}C_{air}$ applied to the samples varied between −8.36‰ and −6.86‰ (period 1940–2014) following [49] (available online at http://web.udl.es/usuaris/x3845331/AIRCO2_LOESS.xls).

Indexed $\Delta^{13}C$ and $\delta^{18}O$ chronologies (hereafter $\Delta^{13}C_i$ and $\delta^{18}O_i$) were obtained following the same procedure used for TRW_i. Both indexed ring-width and isotope chronologies were used as input for climate analyses.

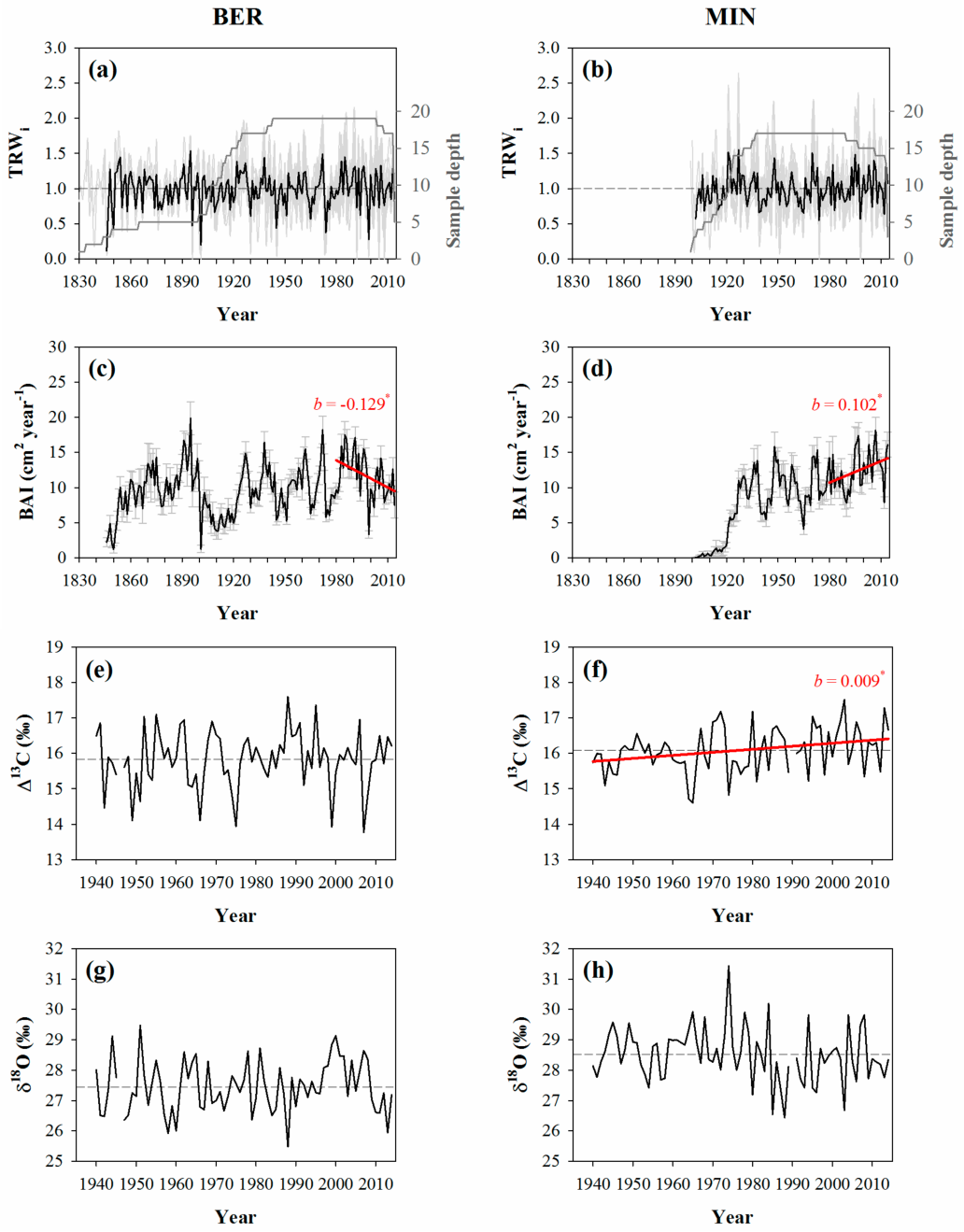

Figure 2. Tree-ring chronologies for BER (left panels) and MIN (right panels). (**a**,**b**) Residual tree-ring width indices (TRW_i) (grey lines) and master chronologies (black lines) for the period when expressed population signal (EPS) exceeded 0.85 (see Table 1). The sampling size for each chronology is indicated by a dark grey line. (**c**,**d**) Mean basal area increment (BAI) calculated from the set of raw TRW series. Error bars denote standard errors. (**e**,**f**) Carbon isotope discrimination ($\Delta^{13}C$) and (**g**,**h**) oxygen isotope composition ($\delta^{18}O$) for the period 1940–2014. Dashed horizontal lines correspond to mean values of tree-ring traits (except BAI). Significant linear trends over time are depicted as red lines (* $p < 0.05$), with the corresponding slope (b) of the trend indicated in each case.

2.4. Intrinsic Water Use Efficiency

Using $\Delta^{13}C$ records, intrinsic water use efficiency (WUE_i) was estimated according to

$$WUE_i = \frac{C_a \times (b - \Delta^{13}C)}{1.6 \times (b - a)} \quad (3)$$

where C_a represents the atmospheric CO_2 concentration, a is the fractioning during diffusion through stomata (~4.4‰) and b is the fractioning during carboxylation by Rubisco and PEP carboxylase (~27‰) [25]. The factor 1.6 denotes the ratio of diffusivities of water vapour and CO_2 in the air. C_a values were taken from the National Oceanic and Atmospheric Administration (NOAA) Earth System Research Laboratory (http://www.esrl.noaa.gov/). We assumed near-constancy of differences between stomatal and internal conductance over time as the high internal conductance of *P. sylvestris* suggests low mesophyll limitations of photosynthesis [50].

In addition, theoretical WUE_i values were calculated according to three scenarios as proposed by [51]. These scenarios describe how the C_i might follow the C_a increase over time: (i) either not at all, when C_i is maintained constant; (ii) in a proportional way, when C_i/C_a is maintained constant; or (iii) at the same rate, when C_a–C_i is maintained constant. Initial C_i values were obtained for each site by applying Equation (3) to the average $\Delta^{13}C$ and C_a values of the first five years of the study period (1940–1944). We used these scenarios to obtain theoretical WUE_i values that were compared to WUE_i records obtained from measured $\Delta^{13}C$. To this end, the sum of squared differences between actual and predicted WUE_i values was divided by the number of observations (years) for each scenario. The square root of this quantity is the root mean square predictive difference (RMS_{PD}), for which smaller values indicated more accurate theoretical predictions.

2.5. Climate Analyses

Long-term series of monthly climate variables (temperature and precipitation) were obtained from the nearest meteorological station to each site (Figure 1a) and covered the period 1940–2014 (with the exception of temperature data for BER, which were available since 1942). In order to quantify drought severity, we estimated the Standardized Precipitation-Evapotranspiration Index (SPEI; [52]) on different time scales (monthly [SPEI1] and May–August [MJJA SPEI4]) using the station climate data. A proxy of water deficit for the growing season (May–August) was also calculated as potential evapotranspiration exceeding precipitation (PET—P), which approximates the water budget on a monthly basis. PET was estimated following [41].

Monthly and seasonal (May–August) mean temperature, precipitation and the SPEI were used to assess the relationships between tree-ring traits and climate for the period 1940–2014. The impact of long-term trends (e.g., global warming) on tree performance was studied by examining tree responses to climate independently for the two halves of the study period (1940–1979 and 1980–2014). The relationships with climate were analyzed through correlation and response functions from the previous October to September of the year of tree-ring formation using the DendroClim2002 program [53]. The significance of function parameters was estimated by drawing 1000 bootstrapped samples with replacement from the initial data set.

2.6. Comparative Evaluation of Scots Pine Responses under Cold–Dry and Warm–Dry Conditions

Our data were complemented with previously compiled records from dry environments typical of warmer regions than the Siberian forest–steppe in which *P. sylvestris* was sampled in two sites of the Gúdar range (Iberian System, eastern Spain) along an altitudinal gradient: mid-altitude (GUD_M, 1615 m a.s.l.) and high-altitude (GUD_H, 2020 m a.s.l.) [37]. These *P. sylvestris* stands are subjected to summer drought, but they differ in thermic regimes: climate is cold–dry in southern Siberia and warm–dry in eastern Spain (Figure 1d,e). The difference in mean annual temperature between these ecosystems is ca. 8 °C, which translates into a more extended growing season in Spain (150 to 180 days

depending on altitude); on the other hand, total precipitation is about two-fold higher in Spain. Altogether, the annual water deficit (PET—P) is about three-fold higher in the Gúdar sites than in those of Central Siberia. Within each region, we distinguished between dry (BER, GUD_M) and relatively wet (moist) conditions (MIN, GUD_H) during the growing season. In this way, we aimed at quantifying the effects of growing conditions (atmospheric CO_2 concentration, climate) on WUE_i and characterized the dependence of BAI on WUE_i changes over time across representative dry environments of this species. The sampling protocol was similar across studies.

Two mixed models testing the assumption of constant responses among stands to selected covariates (i.e., heterogeneity of slopes ANOVA) were fitted to the data over the common period 1980–2011. All variables were first checked for normality (Kolmogorov–Smirnov test) and logarithm-transformed whenever necessary (i.e., BAI). The first model tested for the joint impact of atmospheric CO_2 (C_a) rise and climate (water deficit, WD) on WUE_i. To this end, WUE_i was modelled by introducing the following terms in the model: Region (Siberia, Spain), Site (dry, moist), the interaction of Region × Site, the covariate C_a and its interactions (C_a × Region, C_a × Site and C_a × Region × Site) and the covariate WD (PET—P for the period when mean temperature exceeds 10 °C; [40]) and its interactions (WD × Region, WD × Site and WD × Region × Site). Alternative climatic variables such as temperature or precipitation were not evaluated because they were highly correlated with WD over the study period ($r > 0.55$ for mean temperature; $r > 0.94$ for precipitation, $p < 0.001$ in all cases). WD was preferred over temperature or precipitation because it can be interpreted as an integrative measure of drought severity over the growing season in dry bioclimates [54,55]. The second model explained logarithm-transformed BAI (logBAI) as a function of Region, Site, the interaction Region × Site, the covariate WUE_i and the interactions WUE_i × Region, WUE_i × Site and WUE_i × Region × Site. In both models (WUE_i and logBAI), the tree identity was introduced as subject (random effect), and year was introduced as repeated effect at the tree level with a first-order autoregressive covariance structure to account for temporal autocorrelation. The significance of differences in tree response (slopes) to the selected covariates was further examined by means of the following set of orthogonal contrasts: (i) cold (Siberia) vs. warm (Spain) environments and (ii) dry (BER, GUD_M) vs. moist (MIN, GUD_H) conditions. If second order interactions were significant, independent contrasts for every site were evaluated. All analyses were performed with the MIXED procedure of SAS/STAT software (ver. 9.4, SAS Inc., Cary, NC, USA) using restricted maximum likelihood (REML) for estimation of model parameters. Relationships were considered significant at $p < 0.05$.

3. Results

3.1. Climate Trends

Mean annual temperature increased at a similar rate of ~0.03 °C $year^{-1}$ in BER and MIN for the period 1940–2014 (Figure 3a,b). There was also a steady increase in annual precipitation, but only in MIN ($b = 0.93$ mm $year^{-1}$) (Figure 3a,b). Changes in climate records during the growing season were not consistent across sites. Particularly, mean May–August temperature significantly increased by 0.4 °C from the first to the second half of the study period (1940–1979 and 1980–2014) in BER ($p < 0.05$; two-tailed Student's *t*-test), but remained approximately constant in MIN (Figure 3c,d). On the other hand, May–August precipitation significantly increased by 22 mm during the latter period in MIN ($p < 0.05$) (Figure 3c,d). Altogether, drier growing seasons became marginally more frequent after 1980 in BER according to MJJA SPEI4 (Wilcoxon rank test, $p = 0.08$), suggesting an intensifying impact of warming-induced drought stress which was especially noticeable at the turn of this century (Figure 3e). On the other hand, no relevant changes in SPEI4 were observed in MIN (Figure 3f).

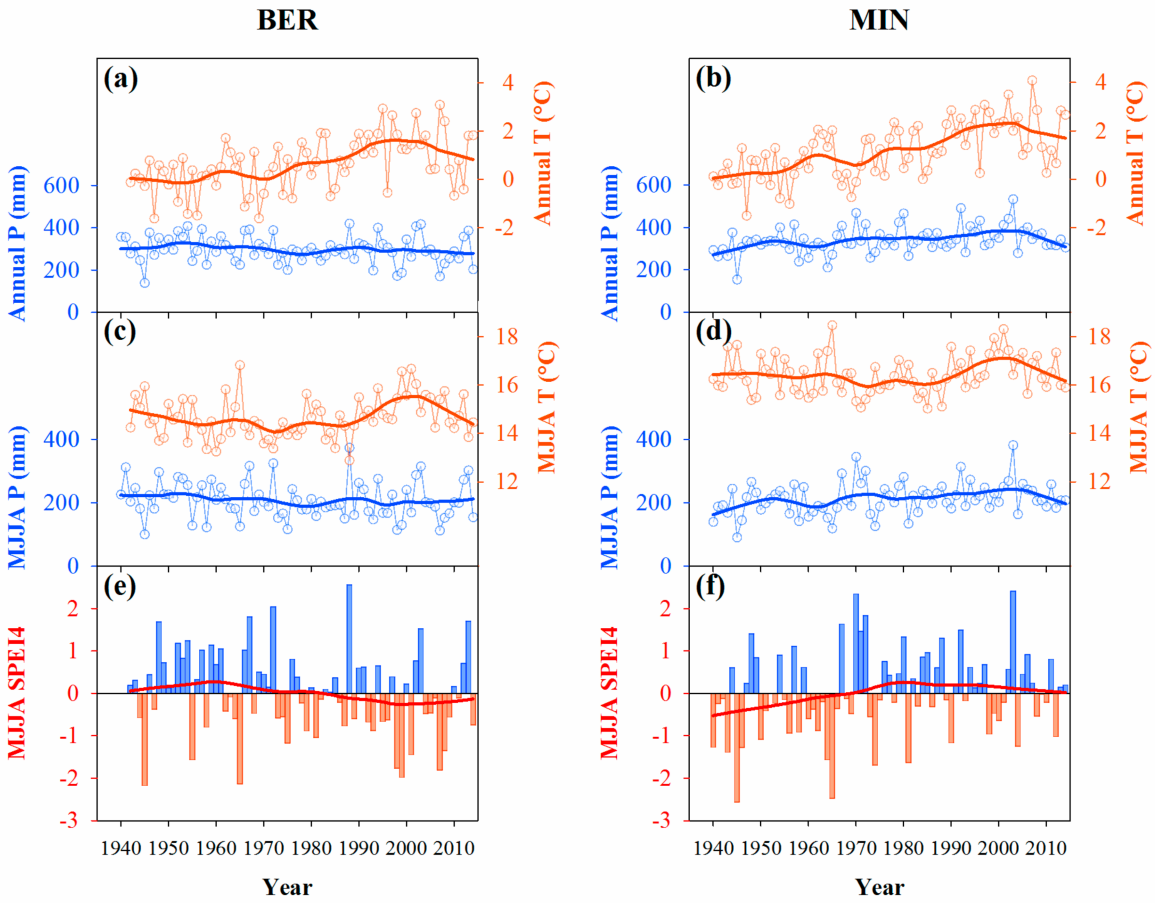

Figure 3. Regional climate trends in BER (left panels) and MIN (right panels) for the period 1940–2014. (**a**,**b**) Annual (upper panels) and (**c**,**d**) growing season (May–August; middle panels) long-term changes in total precipitation (blue lines) and mean temperature (orange lines). The data were obtained from the nearest meteorological station to each sampling site (Shira station for BER; Minusinsk station for MIN). (**e**,**f**) Growing season (May–August) Standardized Precipitation-Evapotranspiration Index (MJJA SPEI4). Positive values indicate wet years (blue bars), while negative values correspond to dry years (orange bars). Temporal trends in climate records (thick lines) are smoothed by LOESS fitting (span = 0.25). Significant (positive) linear trends over time were detected in mean annual temperature at both sites (BER: b = 0.03 °C year^{-1}, $p < 0.001$; MIN: b = 0.03 °C year^{-1}, $p < 0.001$) as well as in total annual precipitation at MIN (b = 0.33 mm year^{-1}, $p < 0.01$).

3.2. Characteristics of Tree-Ring Chronologies

Tree-ring width chronologies having EPS over 0.85 spanned a period of 116 years in MIN and 185 years in BER (Table 1; Figure 2a,b). However, we restricted the study to the period of 1940 to 2014 in concord with the availability of climate data and also to avoid potential juvenile effects on tree records. For this period, ring-width chronologies were characterized by a high inter-series correlation (Table 1) and a high common variance captured by the first principal component (PC1 = 46.7% for MIN and 59.0% for BER), which suggested that trees were responding to common external factors (i.e., climate). Mean ring-width was higher in MIN compared with BER (Table 1). Also, there were consistently higher isotope values in MIN than in BER (Table 1). Between trees variability in isotope values was higher in BER than in MIN (mean SD across years = 0.80‰ vs. 0.43‰ for Δ^{13}C; 0.76‰ vs. 0.29‰ for δ^{18}O). In MIN, Δ^{13}C values showed an increasing trend over time (Figure 2f), while no significant trend was found for either Δ^{13}C in BER or δ^{18}O in both sites (Figure 2e,g,h).

Cross-correlations among indexed tree-ring parameters are shown in Table 2. There was a significant and positive relationship between TRW_i and $\Delta^{13}C_i$ at each site, while a negative association was found between TRW_i and $\delta^{18}O_i$. We also found a strong negative association between both isotopes in MIN. There was a good agreement between sites for TRW_i and $\delta^{18}O_i$, while the relationship was non-significant for $\Delta^{13}C_i$.

Table 2. Pearson correlations involving indexed tree-ring traits (TRW_i, $\Delta^{13}C_i$ and $\delta^{18}O_i$) within and between sites for the period 1940–2014. Site codes are as in Table 1. *, $p < 0.05$; **, $p < 0.01$; ***, $p < 0.001$ (non-significant correlation coefficients are indicated in italics).

	BER—TRW_i	**BER—$\Delta^{13}C_i$**	**BER—$\delta^{18}O_i$**	**MIN—TRW_i**	**MIN—$\Delta^{13}C_i$**	**MIN—$\delta^{18}O_i$**
BER—TRW_i	—	0.51 ***	−0.25 *	0.40 ***	0.46 ***	−0.51 ***
BER—$\Delta^{13}C_i$		—	*−0.16*	*0.10*	*0.14*	−0.31 **
BER—$\delta^{18}O_i$			—	−0.29 *	−0.29 *	0.48 ***
MIN—TRW_i				—	0.63 ***	−0.25 *
MIN—$\Delta^{13}C_i$					—	−0.60 ***
MIN—$\delta^{18}O_i$						—

3.3. Relationships with Climate

Growth responses to climate fluctuations were similar at both sites, although the relationships were overall stronger in MIN (Figure 4). TRW_i responded negatively to high May–August temperatures (Figure 4a,b) and was enhanced by previous November and current May–July precipitation (Figure 4c,d). Such reactions resulted in positive growth responses to reduced drought stress (i.e., positive SPEI1) during the growing season, particularly from May to July (Figure 4e,f). For $\Delta^{13}C$, there were positive correlations with July precipitation in BER and May–July precipitation in MIN. There was also a significant (positive) relationship with previous November precipitation in both sites (Figure 4c,d). A strong negative response of $\Delta^{13}C$ to temperature during May–July was observed in MIN (Figure 4b). Overall, there were strong responses to drought (SPEI1) in July in BER and May–August in MIN (Figure 4e,f). The correlations between $\delta^{18}O$ and temperature were positive, with the strongest responses found during May in BER and May–June in MIN, but also during the previous winter–early spring (previous December, current March) at both sites (Figure 4a,b). Also, $\delta^{18}O$ responded negatively to current February and June–July precipitation, and to previous December precipitation in BER and previous November precipitation in MIN (Figure 4c,d). Significant negative associations were found between $\delta^{18}O$ and SPEI1 in May–July (BER) and June–July (MIN) (Figure 4e,f).

Altogether, the climate analysis showed that variability in tree growth and stable isotopes was sensitive to previous late-autumn and, especially, growing season (May–August) conditions, being most responsive to drought index (SPEI) as it integrates both temperature and precipitation signals. However, these relationships showed a recent shift in the case of stable isotopes (Figure S1 in supplementary material). This effect was especially noticeable in BER. Particularly, we found a significant positive correlation between $\Delta^{13}C$ and MJJA SPEI4 since the 1980s ($r = 0.55$, $p < 0.001$) which was lacking in the preceding period. Likewise, the relationship between $\delta^{18}O$ and SPEI4 strengthened recently ($r = -0.34$, $p < 0.05$ before 1980; $r = -0.58$, $p < 0.001$ after 1980). In contrast, the dependence of tree-ring traits on MJJA SPEI4 slightly weakened in MIN (Figure S1).

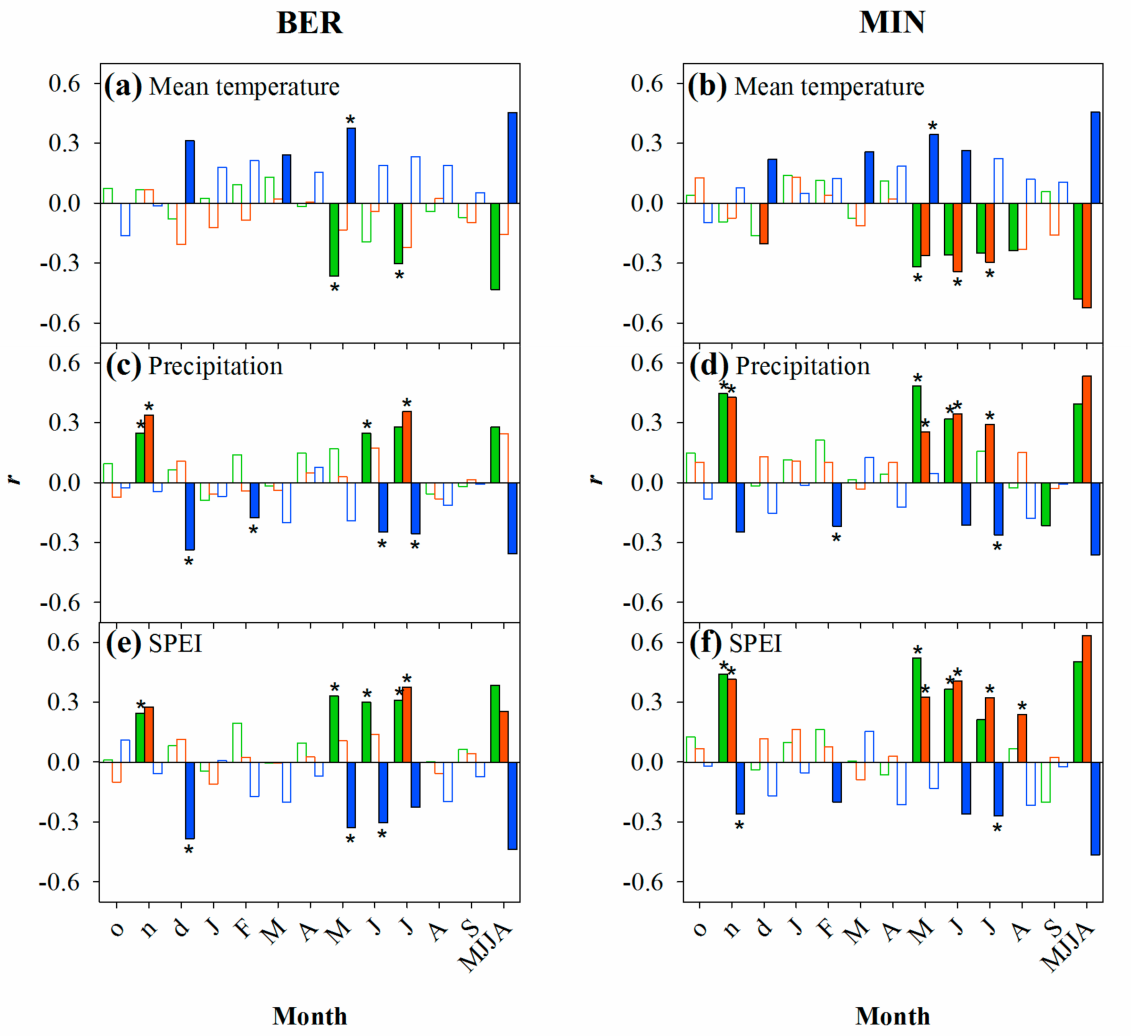

Figure 4. Tree responses to climate in BER (left panels) and MIN (right panels) for the period 1940–2014. The relationships with climate are based on bootstrapped correlations and response function partial regression coefficients between indexed tree-ring data corresponding to each site and (**a**,**b**) mean temperature, (**c**,**d**) precipitation, and (**e**,**f**) Standardized Precipitation-Evapotranspiration Index (SPEI). Climate signals are investigated at monthly and seasonal (May–August) time scales. Significant correlation and partial regression coefficients ($p < 0.05$) are indicated by filled bars and asterisks, respectively. Tree-ring traits are represented in green (TRW_i), orange ($\Delta^{13}C_i$), and blue ($\delta^{18}O_i$). Lowercase and uppercase letters in the *x*-axes correspond to months of the years before and during tree-ring formation, respectively.

3.4. Temporal Dynamics of WUE_i and Relationships with BAI

The mean WUE_i across the period of 1940–2014 was significantly higher in BER (105.3 ± 11.08 µmol mol^{-1}; mean ± SD) than in MIN (102.6 ± 8.54 µmol mol^{-1}) ($p < 0.01$). WUE_i showed increasing trends over time at both sites (Figure 5a,c), ranging from 20% (MIN) to 24% (BER) between the first (1940–1949) and the last decade (2005–2014) of the study period, with decadal increments of 2.9 µmol mol^{-1} (MIN) and 3.6 µmol mol^{-1} (BER). The comparison of temporal trends of $\Delta^{13}C$-based WUE_i records against three WUE_i scenarios (C_i = const.; C_i/C_a = const.; $C_a - C_i$ = const.) indicated higher predictive power of the C_i/C_a= const. scenario at both sites (Figure 5a,c).

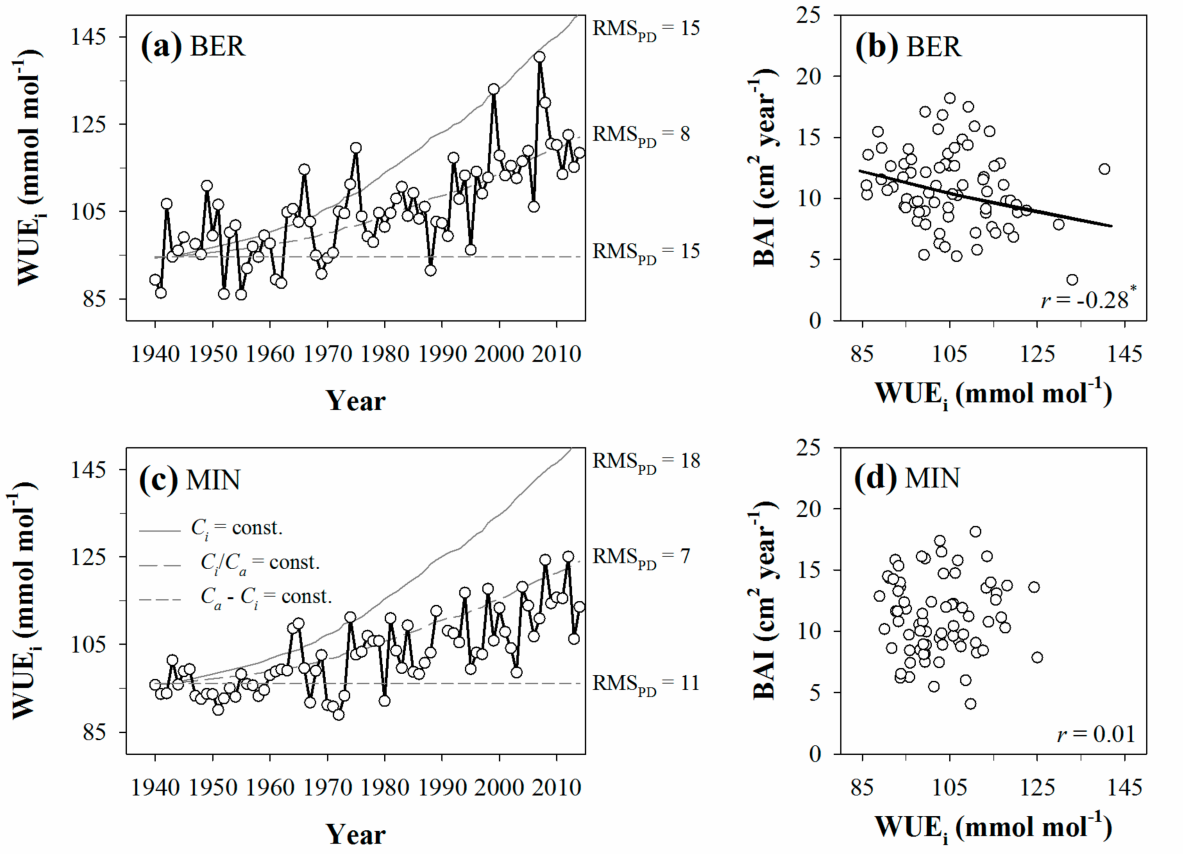

Figure 5. Long-term evolution of intrinsic water use efficiency (WUE_i) and its relationship with basal area increment (BAI) for BER (upper panels) and MIN (lower panels) for the period 1940–2014. (**a**,**c**) Temporal trends in intrinsic water use efficiency (WUE_i) as related to three conceptual models assuming a constant intercellular CO_2 concentration (C_i = const. scenario; solid line), a constant ratio between intercellular and atmospheric CO_2 concentrations (C_i/C_a = const. scenario; long dashed line) and a constant difference between atmospheric and intercellular CO_2 concentrations ($C_a - C_i$ = const. scenario; short dashed line). The root mean square predictive difference (actual minus predicted values; RMS_{PD}) is shown for each model. (**b**,**d**) Relationships between WUE_i and basal area increment (BAI). A significant trend over time is depicted with a black line (*, $p < 0.05$).

The increasing WUE_i trend was accompanied by distinct growth patterns at the site level (Figure 2c,d). Both sites showed a stable BAI from 1940 to 1979 with similar growth rates (10.0 ± 2.97 cm^2 year^{-1} for BER; 9.9 ± 2.88 cm^2 year^{-1} for MIN). After 1980, however, BAI showed a decreasing trend in BER ($b = -0.129$ cm^2 year^{-2}; $p < 0.05$), while it increased in MIN ($b = 0.102$ cm^2 year^{-2}; $p < 0.05$). Changes in long-term radial growth also affected site-level relationships with WUE_i (Figure 5b,d). For the initial period of 1940–1979, there were significantly negative correlations between BAI and WUE_i in BER ($r = -0.50$; $p < 0.01$) and MIN ($r = -0.54$; $p < 0.001$). However, while this association vanished after 1980 in MIN ($r = -0.22$; $p = 0.22$), it strengthened in BER ($r = -0.56$; $p < 0.001$).

3.5. WUE_i and BAI Trends in Cold–Dry (South Central Siberia) and Warm–Dry (Eastern Spain) Environments

WUE_i increased over time at a similar pace regardless of region and site (Figure S2 in supplementary material). In particular, both C_a and WD significantly boosted WUE_i over the last three decades (Figure 6a,b; Table S1 in supplementary material). However, changes in WUE_i due to raising C_a were heterogeneous and depended simultaneously on region and site (dry vs. moist) ($p < 0.001$ for the term C_a × Region × Site) (Table S1). The highest WUE_i increase to rising C_a was found under warm–moist conditions ($b = 0.456$ µmol mol^{-1} ppm^{-1}), followed by cold–dry

(b = 0.340 µmol mol^{-1} ppm^{-1}), cold–moist (b = 0.239 µmol mol^{-1} ppm^{-1}), and warm–dry conditions (b = 0.149 µmol mol^{-1} ppm^{-1}) (Figure 6a). The contrast between warm–moist (GUD_H) and warm–dry (GUD_M) environments showed the most pronounced difference in the response of WUE_i to C_a ($p < 0.001$). On the other hand, there was no significant difference between cold–dry and cold–moist conditions (Figure 6a). In contrast, changes in WUE_i driven by water deficit (WD) were fundamentally due to differences between regions ($p < 0.01$ for the term WD × Region) (Table S1). Hence, WUE_i changes in response to WD were homogeneous within cold (Siberia) and within warm (Spain) environments, being larger (or more reactive to increasing WD) in trees growing in cold (Siberia) than in warm (Spain) conditions (difference = 0.042 µmol mol^{-1} mm^{-1}; $p < 0.01$) (Figure 6b).

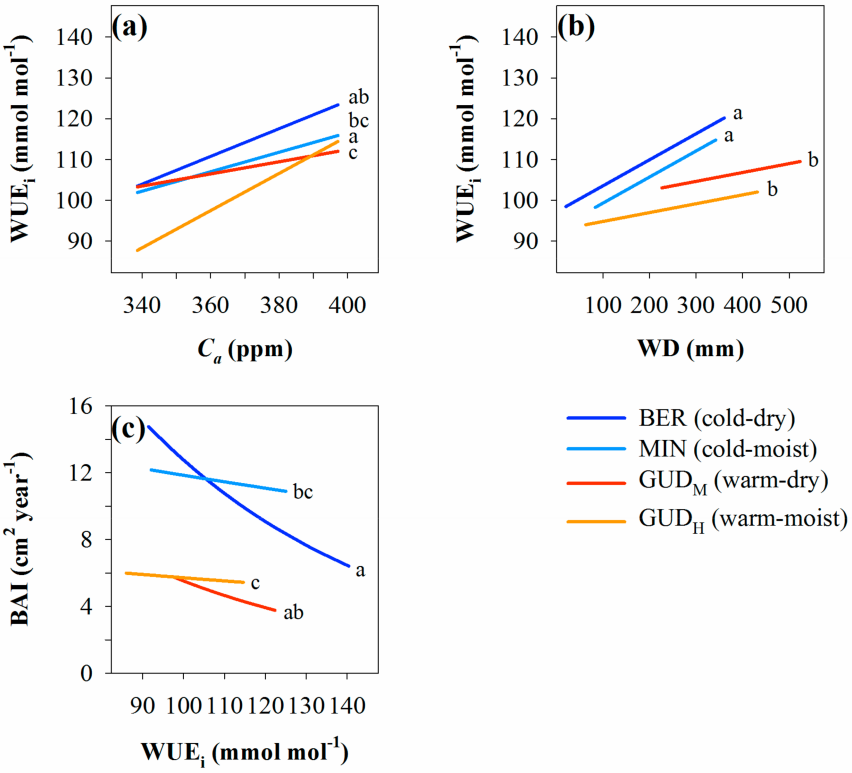

Figure 6. The effects of (**a**) atmospheric CO_2 concentration (C_a) and (**b**) growing season water deficit (WD; evapotranspirative demand exceeding precipitation) on intrinsic water use efficiency (WUE_i) as a function of region (Central Siberia, Eastern Spain) and site (dry, moist). (**c**) The effect of WUE_i on BAI as a function of region and site. For each combination of region and site, different letters indicate significant differences between slopes of responses according to a Student's t-test (α = 0.05).

We also found an overall negative relationship between BAI and WUE_i (Figure 6c). However, the response of BAI to changes in WUE_i depended largely on growing condition ($p < 0.001$ for the term WUE_i × Site) (Table S2 in supplementary material). BAI decreased more strongly in response to enhanced WUE_i under dry than under moist conditions (difference = −0.006 cm^2 year^{-1} µmol^{-1} mol), regardless of region.

4. Discussion

Scots pine growing in the dry forest–steppes of Central Siberia is subjected to severe continentality (summer-winter temperature difference of ca. 40 °C) and scarce annual precipitation (ca. 300 mm) concentrated in summer. The effects of such climate conditions on tree physiology, anatomy, and reaction to climate warming have been fairly less explored [30,31,33] compared with other temperate and boreal regions where this widespread conifer is found. Despite a short and rainy growing season, the studied

Scots pine stands showed a strong interannual dependence on water availability, which indicates that their performance in such cold–dry environments is limited by water shortage rather than by low temperatures. However, the impact of drought elicited contrasting site responses as modulated by the joint effect of local climate and increasing atmospheric CO_2 concentrations over the last 75 years.

4.1. Site Differences in Tree Performance as Indicated by Radial Growth and Stable Isotopes

The good correspondence of ring-width variability between site chronologies, which was slightly lower than that found among series for each chronology, indicates that common factors determine Scots pine growth in the study region. Indeed, the observation that radial growth and $\Delta^{13}C$ were tightly (positively) associated at both sites is expected under frequent and intense drought episodes, since both traits are strongly influenced by water shortage in Scots pine [37,56]. *P. sylvestris* is a conifer with a high stomatal sensitivity to water availability [57]. This isohydric behavior has been supported by strong ^{13}C discrimination in trees subjected to artificial irrigation [58] or sampled across water availability gradients [59,60].

Compared with MIN, pines in the drier but colder site (BER) showed lower radial growth and $\Delta^{13}C$, hence pointing to a greater incidence of drought stress on tree physiology. However, the lower radial growth in BER could be partly related to the fact that trees in BER were about 20 years older on average compared to MIN, so a potential ontogenic effect could have also played a role on such growth differences between sites. Conversely, the higher mean tree-ring $\delta^{18}O$ and the negative temporal association between $\Delta^{13}C$ and $\delta^{18}O$ in MIN seem to contradict a higher water limitation occurring in BER. Thus, the $\delta^{18}O$ results could be understood as the outcome of a higher evaporative enrichment of leaf water mediated by tighter stomatal control in MIN (provided source water is roughly equivalent across sites) [27,61]. On the other hand, the increase in annual and growing season precipitation in MIN is concomitant with the steady $\Delta^{13}C$ increase observed over the study period, whereas a significant relationship between $\Delta^{13}C$ and $\delta^{18}O$ found in BER after 1980 ($r = -0.33$, $p < 0.01$) suggests enhanced stomatal control of water losses under increasing drought stress at this site. Altogether, we interpret these findings as an enhanced carbon uptake in MIN with time, but a higher incidence of drought, hence reducing carbon assimilation, in BER. Most likely, these patterns can be explained owing to the opposite trends observed in climate factors during the growing season for the last 30 years (constant temperature and increasing precipitation in MIN; increasing temperature and constant precipitation in BER).

4.2. Drought Rather than Low Temperatures Determines Long-Term Regional Performance of Scots Pine

Scots pine growth was constrained by low precipitation and high temperatures during the short growing season in the study area. The negative association of growth with warm spring–summer temperatures across sites along with the positive effect of precipitation emphasize the relevance of drought effects on pinewoods in the Siberian dry forest–steppe [31,32]. Conversely, we did not find hints of altered phenology nor of growth limitation by low temperatures during the growing season, as is the case in high altitude or high latitude Scots pine forests [6]. The higher sensitivity to climate found in MIN was probably related to the low water retention and thermal inertia typical of sandy soils, which made Scots pine more responsive to climatic fluctuations at this site. This may also explain the higher stomatal sensitivity observed in MIN according to $\Delta^{13}C$ vs. $\delta^{18}O$ relationships. As suggested by SPEI fluctuations, warmer temperatures led to enhanced evapotranspiration which, in combination with low precipitation, hampered tree growth in such water-limited stands. On the other hand, the positive influence of previous November precipitation can be interpreted in terms of snow cover depth, which protects roots from freeze damage in winter and serves as a source of water early in the growing season [32].

The dependence of radial growth on growing season precipitation has been widely reported in *P. sylvestris* and regarded as independent of temperature regime [30], which mainly determines the length of the growing season. As with most pines, *P. sylvestris* is an opportunistic species highly

responsive to precipitation pulses if water becomes limiting at any moment during growth [58,62]. The prevalence of drought effects over low temperature restrictions on growth suggests that warming-induced water limitation will progressively spread over areas of North Asia—having low precipitation but, also, very low temperatures (i.e., under extreme continentality)—as already observed in Yakutia [56]. Drought effects on Scots pine may not be limited to growth impairment, but they may also hamper the formation of a functional xylem structure via a reduction of cell lumen and wall thickness, as shown for the region [33,63].

The low correspondence between site chronologies for $\Delta^{13}C$ was unexpected since it is usually assumed that carbon isotopes, as surrogates of the tree's carbon and water balance, are better tracers of regional climate variability than ring-width [24,64]. In fact, $\Delta^{13}C$ and ring-width relationships with climate were very similar in MIN (i.e., overlapping), whereas $\Delta^{13}C$ dependence on climate was weaker in BER and concentrated in peak summer (July). Different conditions of moisture supply between sites may have contributed to such differences, with pines in BER being buffered from short-term changes in water availability due to higher soil water retention. Similarly to radial growth, a strong precipitation signal of previous November was also recorded in $\Delta^{13}C$ at both sites, despite the fact that the importance of November precipitation in the annual water budget is very limited (<5% of total precipitation and about 10% of out of season precipitation). This observation is puzzling and anticipates not only a mere protecting role of the first snows to the root system, but also an important function in tree ecophysiology that would deserve careful examination.

Relationships between $\delta^{18}O$ and climate pointed to a mixture of environmental signals. On the one hand, negative associations with SPEI during the growing season suggest a leaf water enrichment signal driven by air humidity that is passed on to the leaf organic matter and readily transferred to the trunk, as supported by a high stomatal sensitivity and fast turnover rates in *P. sylvestris* [65]. On the other hand, $\delta^{18}O$ relationships involving the snowfall season (especially with temperature) indicate a strong signal of meteoric water that was registered in tree rings [66]. Both signal types were quite consistent across sites but winter imprints in tree rings were stronger in BER, in agreement with a higher soil water holding capacity which presumably made pines less dependent on climate vagaries during the growing season.

The recent increase in tree sensitivity to growing season climate in BER confirms an amplifying negative influence of summer drought on tree performance. This is in concord with a decreasing BAI at this site, which is a strong indicator for growth decay since age-related trends in BAI, are overall positive and do not show a decline until trees begin to senesce [46]. On the contrary, the effect of increasing precipitation in MIN seemed to overcome the potentially negative effects of warming, boosting secondary growth (see next section). Indeed, *P. sylvestris* performance under varying water availability is essentially modulated by plastic responses in functional characteristics such as WUE_i [62] or wood anatomy [67], among others.

4.3. Comparable WUE_i Trends but Contrasting BAI Highlight the Relevance of Local Conditions in Forecasting Reactions to Climate

CO_2 and climate are the main drivers of WUE_i variability in Scots pine [68]. An increasing trend in WUE_i of ca. 22% across sites over the last 75 years, which is consistent with an scenario of constant ratio of intercellular to ambient CO_2 concentration, agrees with the general performance of *P. sylvestris* across its distribution range (e.g., Alps mountains [69], central Europe [70] or north-eastern China [71]) (but see [16]). This is in fact the most commonly observed response of forests worldwide to increasing atmospheric CO_2 [51,70,72]. Although WUE_i showed such increasing regional trend, BAI patterns started to drift apart in the 1980s (increasing in MIN, decreasing in BER), in concord with the divergent climate trends observed in the study sites. In any case, BAI and WUE_i were either unrelated (MIN) or negatively related (BER) over the whole study period and, in particular, during the last 35 years. Many studies have also shown lack of CO_2-driven growth stimulation in drought-prone environments

in spite of a recorded increase in WUE_i [73–77]. Instead, increasingly warmer but wetter conditions probably boosted tree growth in MIN from 1980 onwards.

Our findings highlight how subtle changes in local conditions, mediated by CO_2 effects, may differentially impact on radial growth in a transition area between the water-limited grasslands in the south and the temperate mixed forests in the north of central Asia, which is near the trailing edge of the species' distribution in the continent. Here, the particular site balance between low temperature limiting the length of the growing season and scarce summer precipitation limiting tree performance is turning into contrasting growth and physiological responses. This observation was somewhat anticipated in a previous study based on provenance trials [78], in which a reduction in tree height at age 13 of ca. −1% (or −4 cm, that is, almost no change) was forecasted in the nearby site of Yermakovsky (53°00′ N, 94°00′ E) between 1961–1990 and 2030. Scots pine in this cold–dry region was predicted an intermediate reaction to future climate between that forecasted for severely cold-limited, continental sites (with increments of up to +200% in Yakutsk, north-eastern Eurasia) and that for warmer, less continental sites (with decrements of up to −39% in Volgograd, south-eastern Europe) [78]. While the relevance of CO_2 fertilization in our results is discussed below, the incidence of N deposition on tree performance can be considered negligible in the region [79].

4.4. Deciphering Temporal Dynamics in WUE_i and BAI Across Water-Limited Environments

The forest–steppe zone of Central Siberia and the sub-Mediterranean Gúdar mountain range of eastern Spain represent climate extremes where *P. sylvestris* is subjected to recurrent summer droughts (*cf*. Figure 1d,e). In both cases, the radial growth pattern of *P. sylvestris* [80] implies that source (photosynthesis) and sink (xylogenesis) activities are jointly exposed to water shortage in summer. Hence, a relevant question arises about to what extent WUE_i and BAI are (un)coupled in such contrasting thermal regimes. Both areas are subjected to low N deposition [81] and, hence, the observed increases in WUE_i were most likely unrelated to changes in nutrient availability. Conversely, WUE_i trends were simultaneously dependent on atmospheric CO_2 (C_a) and water deficit (WD), as reported elsewhere [68,69].

We found, however, that C_a and WD contributed differentially to changes in WUE_i depending on region and level of water availability. Expressed in relative change over the last 75 years for a site-constant WD, the highest and lowest WUE_i responses to C_a were observed in warm Mediterranean environments (+27% and +7% under moist and dry conditions, respectively), with intermediate values for the cold Siberian sites (+19% and +14% under moist and dry conditions, respectively). The Mediterranean sites represent extreme and opposite reactions to C_a if compared with the mean WUE_i increase due to CO_2 fertilization (ca. 22%) reported for conifers across Europe over the 20th century [82]. With high temperatures, the plasticity of WUE_i responses to C_a was strongly mediated by water availability, in a way that a favorable moisture regime may allow increasing photosynthesis over a long growing season and, hence, exploiting better a progressively larger *C* substrate. This situation was also observed, but to a lesser extent, in cold Siberian sites having a shorter growing period. Notably, the WUE_i dependence on water availability for a site-constant C_a was stronger in Siberia than in Spain, with average WUE_i differences of 19% and 7% between WD extremes, respectively (i.e., almost three-fold higher sensitivity in Siberia). We hypothesize that the shorter growing season in cold–dry environments may have prompted larger differences in gas exchange of Scots pine among years compared with the more extended vegetative period typical of warmer climates, which may allow plastic pines to deal more efficiently with seasonal fluctuations in water availability.

Interestingly, BAI relationships with WUE_i followed site-specific patterns that differed from those observed for WUE_i in its dependence on C_a and WD. The increase in WUE_i did not translate into enhanced growth, but rather the opposite; in particular, BAI decreased more strongly at the driest site of each region (−57% and −35% for Siberia and Spain, respectively) than at its wetter counterparts (−10% and −9%, respectively). In dry areas, high WUE_i rates are associated with the cost of reduced CO_2 assimilation in isohydric conifers such as Scots pine [83], which is beneficial for protecting against

xylem cavitation [84]. Our findings highlight the usefulness of a combined growth–isotope analysis and suggest a predictable pattern of radial growth relationships with WUE_i that would be dependent on the difference in water deficit experienced among stands for the prevailing thermic regime of a region. This assumption would require more data gathered across the dry distribution edge of Scots pine.

5. Conclusions

The forest–steppe ecotone in Central Siberia is subjected to a delicate equilibrium posed by the combined effects of current warming and drought on Scots pine (relaxation of low temperature limitations vs. vulnerability to increasing water shortage), which results in contrasting site performances in terms of growth and physiology. If water availability becomes progressively more limiting, it may tip the balance towards strong reductions in growth rates despite the general increasing trend in WUE_i. Conversely, pinewoods in the region could benefit from CO_2 fertilization if an increase in temperature is accompanied by concomitant increments in precipitation, hence boosting secondary growth. Altogether, our results highlight different fates of Scots pine forests in cold–dry regions as mediated by concurrent changes in atmospheric CO_2 concentration and local climate conditions.

Supplementary Materials: The following are available online at www.mdpi.com/1999-4907/8/12/490/s1, Figure S1: Changes in tree responses to seasonal drought stress (May–August Standardized Precipitation-Evapotranspiration Index) over the two halves of the study period (1940–1979 and 1980–2014); Figure S2: Long-term evolution of intrinsic water use efficiency (WUE_i) of four Scots pine stands located in the forest–steppe zone of Central Siberia (cold sites) and in sub-Mediterranean Eastern Spain (warm sites); Table S1: Significance of fixed effects of linear mixed models with intrinsic water use efficiency (WUE_i) explained as a function of Region, Site, atmospheric CO_2 concentration and growing season water deficit; Table S2: Significance of fixed effects of linear mixed models with basal area increment (logBAI) explained as a function of Region, Site, and intrinsic water use efficiency.

Acknowledgments: This study was funded by the Spanish Government (grant number AGL2015-68274-C3-3-R) and the Russian Science Foundation (project numbers 14-14-00295, sampling and tree-ring data obtainment and 14-14-00219-P, mathematical approach). We acknowledge P. Sopeña and M.J. Pau for technical assistance.

Author Contributions: A.V.K., J.V., and M.S. conceived and designed the experiment; A.V.K. was responsible for field data collection, tree-ring cross-dating, and measurements; M.S. and R.T.W.S. performed isotope analysis; T.A.S. carried out the analyses and led the writing, with substantial contributions from J.V., A.V.K., M.S., and R.T.W.S. All the authors read and approved the final draft of the manuscript.

Conflicts of Interest: The authors declare no conflict of interest.

References

1. Carlisle, A.; Brown, A.H.F. *Pinus sylvestris* L. *J. Ecol.* **1968**, *56*, 269–307. [CrossRef]
2. Matías, L.; Jump, A.S. Interactions between growth, demography and biotic interactions in determining species range limits in a warming world: The case of *Pinus sylvestris*. *For. Ecol. Manag.* **2012**, *282*, 10–22. [CrossRef]
3. Taeger, S.; Fussi, B.; Konnert, M.; Menzel, A. Large-scale genetic structure and drought-induced effects on European Scots pine (*Pinus sylvestris* L.) seedlings. *Eur. J. For. Res.* **2013**, *132*, 481–496. [CrossRef]
4. Gyertich, M. Provenance variation in growth and phenology. In *Genetics of Scots Pine*; Gyertich, M., Mátyás, C., Eds.; Elsevier: Amsterdam, The Netherlands, 1991; pp. 87–101, ISBN 9781483291635.
5. Gervais, B.R.; MacDonald, G.M. A 403-year record of July temperatures and treeline dynamics of *Pinus sylvestris* from the Kola Peninsula, northwest Russia. *Arct. Antarct. Alp. Res.* **2000**, *32*, 295–302. [CrossRef]
6. Briffa, K.R.; Shshov, V.V.; Melvin, T.M.; Vaganov, E.A.; Grudd, H.; Hantemirov, R.M.; Eronen, M.; Naurzbaev, M.M. Trends in recent temperature and radial tree growth spanning 2000 years across northwest Eurasia. *Philos. Trans. R. Soc. B* **2008**, *363*, 2271–2284. [CrossRef] [PubMed]
7. McCarroll, D.; Loader, N.J.; Jalkanen, R.; Gagen, M.H.; Grudd, H.; Gunnarson, B.E.; Kirchhefer, A.J.; Friedrich, M.; Linderholm, H.W.; Lindholm, M.; et al. A 1200-year multiproxy record of tree growth and summer temperature at the northern pine forest limit of Europe. *Holocene* **2013**, *23*, 471–484. [CrossRef]
8. Alisov, B.P. *The Climate of the Soviet Union*; Moscow University Press: Moscow, USSR, 1956; 126p. (In Russian)

9. Bonan, G.B. Forests and climate change: Forcings, feedbacks, and the climate benefits of forests. *Science* **2008**, *320*, 1444–1449. [CrossRef] [PubMed]
10. Choat, B.; Jansen, S.; Brodribb, T.J.; Cochard, H.; Delzon, S.; Bhaskar, R.; Bucci, S.J.; Feild, T.S.; Gleason, S.M.; Hacke, U.G.; et al. Global convergence in the vulnerability of forests to drought. *Nature* **2012**, *491*, 752–755. [CrossRef] [PubMed]
11. Williams, A.P.; Allen, C.D.; Macalady, A.K.; Griffin, D.; Woodhouse, C.A.; Meko, D.M.; Swetnam, T.W.; Rauscher, S.A.; Seager, R.; Grissino-Mayer, H.D.; et al. Temperature as a potent driver of regional forest drought stress and tree mortality. *Nat. Clim. Chang.* **2013**, *3*, 292–297. [CrossRef]
12. Allen, C.D.; Breshears, D.D.; McDowell, N.G. On underestimation of global vulnerability to tree mortality and forest die-off from hotter drought in the Anthropocene. *Ecosphere* **2015**, *6*, 129. [CrossRef]
13. Kullman, L.; Kjällgren, L. Holocene pine tree-line evolution in the Swedish Scandes: Recent tree-line rise and climate change in a long-term perspective. *Boreas* **2006**, *35*, 159–168. [CrossRef]
14. Martínez-Vilalta, J.; Piñol, J. Drought-induced mortality and hydraulic architecture in pine populations of the NE Iberian Peninsula. *For. Ecol. Manag.* **2002**, *161*, 247–256. [CrossRef]
15. Rigling, A.; Bigler, C.; Eilmann, B.; Feldmeyer-Christe, E.; Gimmi, U.; Ginzler, C.; Graf, U.; Mayer, P.; Vacchiano, G.; Weber, P.; et al. Driving factors of a vegetation shift from Scots pine to pubescent oak in dry Alpine forests. *Glob. Chang. Biol.* **2013**, *19*, 229–240. [CrossRef] [PubMed]
16. Hereş, A.M.; Voltas, J.; Claramunt López, B.; Martínez-Vilalta, J. Drought-induced mortality selectively affects Scots pine trees that show limited intrinsic water use efficiency responsiveness to raising atmospheric CO_2. *Funct. Plant Biol.* **2014**, *41*, 244–256. [CrossRef]
17. Pellizzari, E.; Camarero, J.J.; Gazol, A.; Sangüesa-Barreda, G.; Carrer, M. Wood anatomy and carbon-isotope discrimination support long-term hydraulic deterioration as a major cause of drought-induced dieback. *Glob. Chang. Biol.* **2016**, *22*, 2125–2137. [CrossRef] [PubMed]
18. Lloyd, A.H.; Bunn, A.G. Responses of the circumpolar boreal forest to 20th century climate variability. *Environ. Res. Lett.* **2007**, *2*, 045013. [CrossRef]
19. Buermann, W.; Parida, B.R.; Jung, M.; MacDonald, G.M.; Tucker, C.J.; Reichstein, M. Recent shift in Eurasian boreal forest greening response may be associated with warmer and drier summers. *Geophys. Res. Lett.* **2014**, *41*, 1995–2002. [CrossRef]
20. Düthorn, E.; Schneider, L.; Günther, B.; Gläser, S.; Esper, J. Ecological and climatological signals in tree-ring width and density chronologies along a latitudinal boreal transect. *Scand. J. For. Res.* **2016**, *31*, 750–757. [CrossRef]
21. Sánchez-Salguero, R.; Camarero, J.J.; Hevia, A.; Madrigal-González, J.; Linares, J.C.; Ballesteros-Canovas, J.A.; Sánchez-Miranda, A.; Alfaro-Sánchez, R. What drives growth of Scots pine in continental Mediterranean climates: Drought, low temperatures or both? *Agric. For. Meteorol.* **2015**, *206*, 151–162. [CrossRef]
22. Camarero, J.J.; Gazol, A.; Sancho-Benages, S.; Sangüesa-Barreda, G. Know your limits? Climate extremes impact the range of Scots pine in unexpected places. *Ann. Bot.* **2015**, *116*, 917–927. [CrossRef] [PubMed]
23. Babst, F.; Poulter, B.; Bodesheim, P.; Mahecha, M.D.; Frank, D.C. Improved tree-ring archives will support earth-system science. *Nat. Ecol. Evol.* **2017**, *1*, 0008. [CrossRef] [PubMed]
24. McCarroll, D.; Loader, N.J. Stable isotopes in tree rings. *Quat. Sci. Rev.* **2004**, *23*, 771–801. [CrossRef]
25. Farquhar, G.D.; Ehleringer, J.; Hubick, K. Carbon isotope discrimination and photosynthesis. *Annu. Rev. Plant Physiol. Plant Mol. Biol.* **1989**, *40*, 503–537. [CrossRef]
26. Yakir, D. Variations in the natural abundances of oxygen-18 and deuterium in plant carbohydrates. *Plant Cell Environ.* **1992**, *15*, 1005–1020. [CrossRef]
27. Scheidegger, Y.; Saurer, M.; Bahn, M.; Siegwolf, R.T.W. Linking stable oxygen and carbon isotopes with stomatal conductance and photosynthetic capacity: A conceptual model. *Oecologia* **2000**, *125*, 350–357. [CrossRef] [PubMed]
28. Barbour, M.M.; Walcroft, A.S.; Farquhar, G.D. Seasonal variation in $\delta^{13}C$ and $\delta^{18}O$ of cellulose from growth rings of *Pinus radiata*. *Plant Cell Environ.* **2002**, *25*, 1483–1499. [CrossRef]
29. Barnard, H.R.; Brooks, J.R.; Bond, B.J. Applying the dual-isotope conceptual model to interpret physiological trends under controlled conditions. *Tree Physiol.* **2012**, *32*, 1183–1198. [CrossRef] [PubMed]
30. Rigling, A.; Waldner, P.O.; Forster, T.; Bräker, O.U.; Pouttu, A. Ecological interpretation of tree-ring width and intraannual density fluctuations in *Pinus sylvestris* on dry sites in the central Alps and Siberia. *Can. J. For. Res.* **2001**, *31*, 18–31. [CrossRef]

31. Wu, X.; Liu, H.; Guo, D.; Anenkhonov, O.A.; Badmaeva, N.K.; Sandanov, D.V. Growth decline linked to warming-induced water limitation in hemi-boreal forests. *PLoS ONE* **2012**, *8*, e42619. [CrossRef] [PubMed]
32. Babushkina, E.A.; Vaganov, E.A.; Belokopytova, L.V.; Shishov, V.V.; Grachev, A.M. Competitive strength effect in the climate response of Scots pine radial growth in south-Central Siberia forest–steppe. *Tree Ring Res.* **2015**, *71*, 106–117. [CrossRef]
33. Fonti, P.; Babushkina, E.A. Tracheid anatomical responses to climate in a forest–steppe in Southern Siberia. *Dendrochronologia* **2016**, *39*, 32–41. [CrossRef]
34. Knorre, A.A.; Siegwolf, R.T.W.; Saurer, M.; Sidorova, O.V.; Vaganov, E.A.; Kirdyanov, A.V. Twentieth century trends in tree ring stable isotopes (δ^{13}C and δ^{18}O) of *Larix sibirica* under dry conditions in the forest steppe in Siberia. *J. Geophys. Res.* **2010**, *115*, G03002. [CrossRef]
35. Soja, A.J.; Tchebakova, N.M.; French, N.H.F.; Flannigan, M.D.; Shugart, H.H.; Stocks, B.J.; Sukhinin, A.I.; Parfenova, E.I.; Chapin, F.S., III; Stackhouse, P.W., Jr. Climate-induced boreal forest change: Predictions versus current observations. *Glob. Planet. Chang.* **2007**, *56*, 274–296. [CrossRef]
36. Tchebakova, N.M.; Parfenova, E.I.; Soja, A.J. Climate change and climate-induced hot spots in forest shifts in central Siberia from observed data. *Reg. Environ. Chang.* **2011**, *11*, 817–827. [CrossRef]
37. Shestakova, T.A.; Camarero, J.J.; Ferrio, J.P.; Knorre, A.A.; Gutiérrez, E.; Voltas, J. Increasing drought effects on five European pines modulate Δ^{13}C-growth coupling along a Mediterranean altitudinal gradient. *Funct. Ecol.* **2017**, *31*, 1359–1370. [CrossRef]
38. Smelansky, I.E.; Tishkov, A.A. The steppe biome in Russia: Ecosystem services, conservation status, and actual challenges. In *Eurasian Steppes. Ecological Problems and Livelihoods in a Changing World, Plant and Vegetation*; Werger, M.J.A., van Staalduinen, M.A., Eds.; Springer: Dordrecht, The Netherlands, 2012; pp. 45–101, ISBN 9789400738867.
39. Critchfield, W.B.; Little, E.L., Jr. *Geographic Distribution of the Pines of the World*; U.S. Department of Agriculture, Forest Service: Washington, DC, USA, 1966; 97p.
40. Swidrak, I.; Gruber, A.; Kofler, W.; Oberhuber, W. Effects of environmental conditions on onset of xylem growth in *Pinus sylvestris* under drought. *Tree Physiol.* **2011**, *31*, 483–493. [CrossRef] [PubMed]
41. Hargreaves, G.H.; Samani, Z.A. Estimating potential evapotranspiration. *J. Irrig. Drain. Div.* **1982**, *108*, 225–230.
42. Holmes, R.L. Computer-assisted quality control in tree-ring dating and measurement. *Tree Ring Bull.* **1983**, *43*, 69–78.
43. Cook, E.R.; Kairiukstis, L.A. *Methods of Dendrochronology: Applications in the Environmental Sciences*; Springer: Dordrecht, The Netherlands, 1990; 394p. ISBN 9789401578790.
44. Cook, E.R.; Krusic, P.J. *Program ARSTAN: A Tree-Ring Standardization Program Based on Detrending and Autoregressive Time Series Modeling, with Interactive Graphics*; Columbia University: Palisades, NY, USA, 2005; p. 14.
45. Wigley, T.M.L.; Briffa, K.R.; Jones, P.D. On the average of correlated time series, with applications in dendroclimatology and hydrometeorology. *J. Clim. Appl. Meteorol.* **1984**, *23*, 201–213. [CrossRef]
46. Biondi, F.; Qeadan, F. A theory-driven approach to tree-ring standardization: Defining the biological trend from expected basal area increment. *Tree Ring Res.* **2008**, *64*, 81–96. [CrossRef]
47. Leavitt, S.W. Tree-ring isotopic pooling without regard to mass: No difference from averaging δ^{13}C values of each tree. *Chem. Geol.* **2008**, *252*, 52–55. [CrossRef]
48. Ferrio, J.P.; Voltas, J. Carbon and oxygen isotope ratios in wood constituents of *Pinus halepensis* as indicators of precipitation, temperature and vapor pressure deficit. *Tellus B Chem. Phys. Meteorol.* **2005**, *57*, 164–173. [CrossRef]
49. Ferrio, J.P.; Araus, J.L.; Buxó, R.; Voltas, J.; Bort, J. Water management practices and climate in ancient agriculture: Inferences from the stable isotope composition of archaeobotanical remains. *Veg. Hist. Archaeobot.* **2005**, *14*, 510–517. [CrossRef]
50. Veromann-Jürgenson, L.L.; Tosens, T.; Laanisto, L.; Niinemets, Ü. Extremely thick cell walls and low mesophyll conductance: Welcome to the world of ancient living! *J. Exp. Bot.* **2017**, *68*, 1639–1653. [CrossRef] [PubMed]
51. Saurer, M.; Siegwolf, R.; Schweingruber, F. Carbon isotope discrimination indicates improving water use efficiency of trees in northern Eurasia over the last 100 years. *Glob. Chang. Biol.* **2004**, *10*, 2109–2120. [CrossRef]

52. Vicente-Serrano, S.M.; Beguería, S.; López-Moreno, J.I. A multi-scalar drought index sensitive to global warming: The Standardized Precipitation Evapotranspiration Index. *J. Clim.* **2010**, *23*, 1696–1718. [CrossRef]
53. Biondi, F.; Waikul, K. DENDROCLIM 2002: A C++ program for statistical calibration of climate signals in tree-ring chronologies. *Comput. Geosci.* **2004**, *30*, 303–311. [CrossRef]
54. United Nations Educational, Scientific and Cultural Organization (UNESCO). *Map of the World Distribution of Arid Regions: Explanatory Note*; UNESCO: Paris, France, 1979; p. 54, ISBN 9789231014840.
55. Le Houerou, H.N. An agro-bioclimatic classification of arid and semiarid lands in the isoclimatic Mediterranean zones. *Arid Land Res. Manag.* **2004**, *18*, 301–346. [CrossRef]
56. Kagawa, A.; Naito, D.; Sugimoto, A.; Maximov, T.C. Effects of spatial variability in soil moisture on widths and $\delta^{13}C$ values of eastern Siberian tree rings. *J. Geophys. Res.* **2003**, *108*, 4500. [CrossRef]
57. Irvine, J.; Perks, M.P.; Magnani, F.; Grace, J. The response of *Pinus sylvestris* to drought: Stomatal control of transpiration and hydraulic conductance. *Tree Physiol.* **1998**, *18*, 393–402. [CrossRef] [PubMed]
58. Eilmann, B.; Buchmann, N.; Siegwolf, R.; Saurer, M.; Cherubini, P.; Rigling, A. Fast response of Scots pine to improved water availability reflected in tree-ring width and $\delta^{13}C$. *Plant Cell Environ.* **2010**, *33*, 1351–1360. [CrossRef] [PubMed]
59. Arneth, A.; Lloyd, J.; Šantrůčková, H.; Bird, M.; Grigoryev, S.; Kalaschnikov, Y.N.; Gleixner, G.; Schulze, E.D. Response of central Siberian Scots pine to soil water deficit and long-term trends in atmospheric CO_2 concentration. *Glob. Biogeochem. Cycles* **2002**, *16*, 1005. [CrossRef]
60. Andreu-Hayles, L.; Planells, O.; Gutiérrez, E.; Muntan, E.; Helle, G.; Anchukaitis, K.J.; Schleser, G.H. Long tree-ring chronologies reveal 20th century increases in water use efficiency but no enhancement of tree growth at five Iberian pine forests. *Glob. Chang. Biol.* **2011**, *17*, 2095–2112. [CrossRef]
61. Barbour, M.M. Stable oxygen isotope composition of plant tissue: A review. *Funct. Plant Biol.* **2007**, *34*, 83–94. [CrossRef]
62. Feichtinger, L.M.; Siegwolf, R.T.W.; Gessler, A.; Buchmann, N.; Lévesque, M.; Rigling, A. Plasticity in gas-exchange physiology of mature Scots pine and European larch drive short- and long-term adjustments to changes in water availability. *Plant Cell Environ.* **2017**, *40*, 1972–1983. [CrossRef] [PubMed]
63. Camarero, J.J.; Fernández-Pérez, L.; Kirdyanov, A.V.; Shestakova, T.A.; Knorre, A.A.; Kukarskih, V.V.; Voltas, J. Minimum wood density of conifers portrays changes in early season precipitation at dry and cold Eurasian regions. *Trees* **2017**, *31*, 1423–1437. [CrossRef]
64. Andreu, L.; Planells, O.; Gutiérrez, E.; Helle, G.; Schleser, G.H. Climatic significance of tree-ring width and $\delta^{13}C$ in a Spanish pine forest network. *Tellus B* **2008**, *60*, 771–781. [CrossRef]
65. Gessler, A.; Brandes, E.; Buchmann, N.; Helle, G.; Rennenberg, H.; Barnard, R.L. Tracing carbon and oxygen isotope signals from newly assimilated sugars in the leaves to the tree-ring archive. *Plant Cell Environ.* **2009**, *32*, 780–795. [CrossRef] [PubMed]
66. Sarris, D.; Siegwolf, R.; Körner, C. Inter- and intra-annual stable carbon and oxygen isotope signals in response to drought in Mediterranean pines. *Agric. For. Meteorol.* **2013**, *168*, 59–68. [CrossRef]
67. Eilmann, B.; Zweifel, R.; Buchmann, N.; Fonti, P.; Rigling, A. Drought-induced adaptation of the xylem in Scots pine and pubescent oak. *Tree Physiol.* **2009**, *29*, 1011–1020. [CrossRef] [PubMed]
68. Fernández de Uña, L.; Cañellas, I.; Gea-Izquierdo, G. Stand competition determines how different tree species will cope with a warming climate. *PLoS ONE* **2015**, *10*, e0122255. [CrossRef] [PubMed]
69. Lévesque, M.; Rigling, A.; Bugmann, H.; Webera, P.; Branga, P. Growth response of five co-occurring conifers to drought across a wide climatic gradient in Central Europe. *Agric. For. Meteorol.* **2014**, *197*, 1–12. [CrossRef]
70. Saurer, M.; Spahni, R.; Frank, D.C.; Joos, F.; Leuenberger, M.; Loader, N.J.; McCarroll, D.; Gagen, M.; Poulter, B.; Siegwolf, R.T.W.; et al. Spatial variability and temporal trends in water use efficiency of European forests. *Glob. Chang. Biol.* **2014**, *20*, 332–336. [CrossRef] [PubMed]
71. Zhang, X.; Liu, X.; Zhang, Q.; Zeng, X.; Xu, G.; Wu, G.; Wang, W. Species-specific tree growth and intrinsic water use efficiency of Dahurian larch (*Larix gmelinii*) and Mongolian pine (*Pinus sylvestris* var. *mongolica*) growing in a boreal permafrost region of the Greater Hinggan Mountains, Northeastern China. *Agric. For. Meteorol.* **2018**, *248*, 145–155. [CrossRef]
72. Li, D.; Fang, K.; Li, Y.; Chen, D.; Liu, X.; Dong, Z.; Zhou, F.; Guo, G.; Shi, F.; Xu, C.; et al. Climate, intrinsic water use efficiency and tree growth over the past 150 years in humid subtropical China. *PLoS ONE* **2017**, *12*, e0172045. [CrossRef] [PubMed]

73. Linares, J.C.; Delgado-Huertas, A.; Camarero, J.J.; Merino, J.; Carreira, J.A. Competition and drought limit the water use efficiency response to rising atmospheric CO_2 in the Mediterranean fir *Abies pinsapo*. *Oecologia* **2009**, *161*, 611–624. [CrossRef] [PubMed]
74. Maseyk, K.; Hemming, D.; Angert, A.; Leavitt, S.W.; Yakir, D. Increase in water use efficiency and underlying processes in pine forests across a precipitation gradient in the dry Mediterranean region over the past 30 years. *Oecologia* **2011**, *167*, 573–585. [CrossRef] [PubMed]
75. Peñuelas, J.; Canadell, J.G.; Ogaya, R. Increased water use efficiency during the 20th century did not translate into enhanced tree growth. *Glob. Ecol. Biogeogr.* **2011**, *20*, 597–608. [CrossRef]
76. Battipaglia, G.; De Micco, V.; Brand, W.A.; Saurer, M.; Aronne, G.; Linke, P.; Cherubini, P. Drought impact on water use efficiency and intra-annual density fluctuations in Erica arborea on Elba (Italy). *Plant Cell Environ.* **2014**, *37*, 382–391. [CrossRef] [PubMed]
77. Moreno-Gutiérrez, C.; Battipaglia, G.; Cherubini, P.; Delgado Huertas, A.; Querejeta, J.I. Pine afforestation decreases the long-term performance of understorey shrubs in a semi-arid Mediterranean ecosystem: A stable isotope approach. *Funct. Ecol.* **2015**, *29*, 15–25. [CrossRef]
78. Rehfeldt, G.E.; Tchebakova, N.M.; Parfenova, Y.I.; Wykoff, W.R.; Kuzmina, N.A.; Milyutin, L.I. Intraspecific responses to climate in Pinus sylvestris. *Glob. Chang. Biol.* **2011**, *8*, 912–929. [CrossRef]
79. Fleischer, K.; Wårlind, D.; van der Molen, M.K.; Rebel, K.T.; Arneth, A.; Erisman, J.W.; Wassen, M.J.; Smith, B.; Gough, C.M.; Margolis, H.A.; et al. Low historical nitrogen deposition effect on carbon sequestration in the boreal zone. *J. Geophys. Res.* **2015**, *120*, 2542–2561. [CrossRef]
80. Rossi, S.; Deslauriers, A.; Griçar, J.; Seo, J.W.; Rathgeber, C.B.K.; Anfodillo, T.; Morin, H.; Levanic, T.; Oven, P.; Jalkanen, R. Critical temperatures for xylogenesis in conifers of cold climates. *Glob. Ecol. Biogeogr.* **2008**, *17*, 696–707. [CrossRef]
81. Fernández-Martínez, M.; Vicca, S.; Janssens, I.A.; Sardans, J.; Luyssaert, S.; Campioli, M.; Chapin, F.S., III; Ciais, P.; Malhi, Y.; Obersteiner, M.; Papale, D.; et al. Nutrient availability as the key regulator of global forest carbon balance. *Nat. Clim. Chang.* **2014**, *4*, 471–476. [CrossRef]
82. Frank, D.C.; Poulter, B.; Saurer, M.; Esper, J.; Huntingford, C.; Helle, G.; Treydte, K.; Zimmermann, N.E.; Schleser, G.H.; Ahlström, A.; et al. Water use efficiency and transpiration across European forests during the Anthropocene. *Nat. Clim. Chang.* **2015**, *5*, 579–584. [CrossRef]
83. Martínez-Sancho, E.; Dorado-Liñán, I.; Gutiérrez-Merino, E.; Matiu, M.; Helle, G.; Heinrich, I.; Menzel, A. Increased water use efficiency translates into contrasting growth patterns of Scots pine and sessile oak at their southern distribution limits. *Glob. Chang. Biol.* **2017**. [CrossRef] [PubMed]
84. Körner, C. Paradigm shift in plant growth control. *Curr. Opin. Plant Biol.* **2015**, *25*, 107–114. [CrossRef] [PubMed]